Dynamic Loads Caused By Freight Trains With Wheelset Loads of 250 kN

I. R. Göbel
Federal Institute for Geosciences and Natural Resources (BGR), Hannover, Germany

H. Meyer
State Geological Survey of Lower Saxony (NLfB), Hannover, Germany

ABSTRACT: Increasing wheelset loads of freight trains to 250 kN leads to the question of whether the additional dynamic loads on the track are permissible. Moreover, the operating company (DB, German Railways) was interested in any differences of dynamic load caused by 2 axle and 3 axle bogies with their respective maximum axle loads. Dynamic loads on tracks consist of a low-frequency part caused by train geometry and train velocity, and a high-frequency part due to additional stochastic loads caused by irregularities of wheels, rails, etc. We performed seismic measurements during the passage of ore trains at track sections in Northern Germany where wagons with two and three axles per bogie were in use. Additionally, parameter studies with a Winkler beam model allowed comparison of the low-frequency behaviour of both types of wagon regarding particle velocity and displacement. The measurements are used to estimate the stochastic loads after filtering. The total load on track and subsoil caused by wagons with 6 axles and wheelset loads of 250 kN is compared with wagons with 4 axles and wheelset loads of 225 kN travelling at the same train speed.

KEY WORDS: Energy balance, damage criteria, deterministic load, stochastic load, Winkler beam

1 INTRODUCTION

To further the development of criteria describing damage, decay, and failure of railway tracks, especially tracks on soft soils and loaded by freight trains with high axle loads, we analysed the movements caused by the passage of trains. We distinguish between deterministic and stochastic loads, whereby the former are in the low-frequency range, whereas the latter are mostly in the high-frequency range. Deterministic loads are caused by the train geometry, axle loads, and velocity. Stochastic loads are either due to length-dependent irregularities of the train or track, or caused by irregularities in the movement of the train, such as rolling, heaving, or pitching. Measurements of vibrations at the footing of the ballast are high and low-pass filtered to provide an approximate separation of the two types of loads.

The energy balance of the vertical track movement is determined using the model of a Winkler beam with a moving load. Parameter studies for a single load and wagons with 2 and 3 axle bogies respectively, show the energy transfer for the deterministic loads. Energy analysis of measured vibrations reveals the energy transfer in the real system, especially the ratio of the deterministic and stochastic energy portions.

Finally, the set of data is used to estimate the additional dynamic load caused by the stochastic loading and these results are then compared with values currently used for the dimensioning of tracks (Deutsche Bundesbahn 1992).

2 SYSTEM ANALYSIS OF VIBRATIONS CAUSED BY TRAIN PASSAGE

Basically, the loads and the subsequent vibrations in the track and subsoil caused by the passage of trains can be approximately separated into low and high frequency portions. Deterministic loads are low-frequency and caused by the train geometry, axle loads, and velocity. Stochastic loads are high-frequency and caused by irregularities of train or track, either length dependent or related to irregular movement of the train (Lieberenz et al. 2002). Figure 1 shows the frequencies of typical length dependent deterministic and stochastic features for a particular velocity. Except for rail welds and wheel out-of-roundness, the regular and irregular features belong to different frequency ranges.

We assume that both types of vibrations can be added to each other, e.g.

$$v_{tot} = v_d + v_s \quad (1)$$

where v is the particle velocity. The indices tot, d, and s stand for total, deterministic, and stochastic. The same equation holds for deflections and accelerations.

The deterministic particle velocity v_d is determined from measurements with low-pass filtering with a cut-off frequency of 15 Hz. The stochastic particle velocity v_s results from a high-pass filtering of the measured time series at the same cut-off frequency.

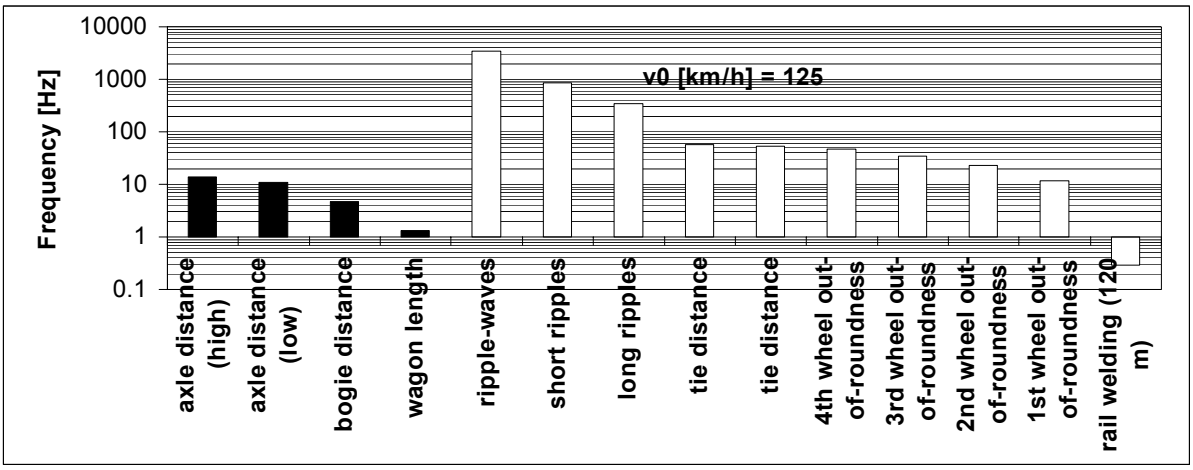

Figure 1: Frequency-distribution of typical length and velocity dependent loads, shown for a train velocity of 125 km/h; black bars: deterministic loads, white bars: stochastic loads. Lengths are mainly given by Lieberenz et al (2002).

3 IN SITU MEASUREMENTS

Geophones are installed along the track at the foot of the ballast, embedded in the subgrade at a depth of about 0.2 m to achieve a good coupling between the ground and the geophones. The distance between the geophones and the middle axis of the track is about 1.5 m. The vertical component of the displacement velocity is measured during the passage of trains.

4 ENERGY BALANCE OF VIBRATIONS

The energy transfer of a train (or moving load) on a track in the vertical direction comprises kinetic energy, E_{kin}, two types of potential energy, E_{pot}, i.e. energy stored in the beam (index B) caused by deflection, and energy stored in the subgrade (index K), and dissipation, ϕ:

$$E_{tot}^{vertical} = E_{kin} + E_{pot}^{K} + E_{pot}^{B} + \phi \quad (2)$$

The four energy components correspond to the four components in the differential equation of the Winkler beam, see next section. The dissipation term is dropped. Hence, when the train velocity is constant, equation (2) is a conservation equation.

We also distinguish between energy terms caused by deterministic and stochastic loads. Please note that while deterministic and stochastic deflection, particle velocity or acceleration add up, energy portions do not, e.g.

$$E_{kin} = E_{kin}^{d} + E_{kin}^{s} + \text{mixed terms} \quad (3)$$

4.1 Winkler Beam Model

We simulate the railway track with the underlying soil with an elastic beam of infinite length on a Winkler foundation, where the Bernoulli beam corresponds to the track with the rails and ballast, and in some cases an embankment. The equation of motion

$$EI\frac{\partial^4 w}{\partial x^4} + \rho A\frac{\partial w^2}{\partial t^2} + 2\delta\frac{\partial w}{\partial t} + K w = P\cdot d(x - v_0 t) \quad (4)$$

has been solved by Fryba (1999) and Dörr (1948). The parameter w is the vertical beam displacement. The beam is characterised by the flexural rigidity, EI, and the mass per unit length, ρA; 2δ is the damping modulus, and K the subgrade reaction modulus. P is a point load moving at constant speed, v_0, along a horizontal axis x; d is the Dirac function, t the time.

4.2 Energy Balance of the Winkler Beam Model

The analytical solution for an individual moving load (Fryba 1999) is applied. With the dimensionless co-ordinate s

$$s = \frac{x - v_0 t}{L_0} \quad \text{with} \quad L_0 = \left(\frac{4EI}{K}\right)^{1/4} \quad (5)$$

we get for the change in kinetic energy:

$$\frac{dE_{kin}}{ds} = \frac{1}{2}\cdot\rho A\cdot\left\{\frac{dw(s)}{dt}\right\}^2 \quad (6)$$

After integration, we have:

$$E_{kin} = \frac{1}{2}\cdot\rho A\cdot\int\left\{\frac{dw(s)}{dt}\right\}^2 ds + C \quad (7)$$

To arrive at the energy (dimension Nm), the integral over the bending line is needed. Using the substitution method,

$$\int f(s)\, ds = \int f(x)\,\frac{ds}{dx}\,dx \quad (8)$$

and using equation (5), we have for t = 0, i.e. at a specific point in time

$$\frac{ds}{dx} = \frac{1}{L_0} \quad (9)$$

From this follows:

$$L_0 \int f(s)\ ds \quad = \quad \int f(x)\,dx \tag{10}$$

Hence, we integrate over s and multiply the result by L_0. The result for frictionless movement and $s < 0$ is:

$$E_{kin} \quad = \quad L_0 \cdot \frac{A_0{}^2 b^2}{8} \cdot \frac{2\rho A \cdot v_0{}^2}{L_0{}^2} \cdot e^{2b\frac{x}{L_0}} \cdot \left\{ \frac{2}{b} - b \cdot \cos\left(2a\frac{x}{L_0}\right) - a \cdot \sin\left(2a\frac{x}{L_0}\right) \right\} \tag{11}$$

For the change in potential energy caused by transfer in the subgrade,

$$\frac{dE_{pot}^K}{ds} \quad = \quad \frac{1}{2} \cdot K \cdot w(s)^2 \tag{12}$$

applies. For the change in potential energy caused by deformation of the beam the following equation holds:

$$\frac{dE_{pot}^B}{ds} \quad = \quad \frac{1}{2} \cdot \frac{M^2}{EI} \quad = \quad \frac{L_0{}^8 K^2}{32EI \cdot v_0{}^4} \cdot \left\{ \frac{d^2 w(s)}{dt^2} \right\}^2 \tag{13}$$

From this the energy stored in the subgrade is:

$$E_{pot}^K = L_0 \cdot \frac{A_0{}^2 b^2}{8} \cdot K \cdot e^{2b\frac{x}{L_0}} \cdot \left\{ \frac{2}{b} + b\left(1+2\alpha^2\right) \cdot \cos\left(2a\frac{x}{L_0}\right) - a\left(1-2\alpha^2\right) \cdot \sin\left(2a\frac{x}{L_0}\right) \right\} \tag{14}$$

The following applies for deformation energy in the beam:

$$E_{pot}^B \quad = \quad L_0 \cdot \frac{A_0{}^2 b^2}{8} \cdot \frac{L_0{}^4 K^2}{4EI} \cdot e^{2b\frac{x}{L_0}} \cdot \left\{ \frac{2}{b} - b \cdot \cos\left(2a\frac{x}{L_0}\right) + a \cdot \sin\left(2a\frac{x}{L_0}\right) \right\} \tag{15}$$

We apply the abbreviations

$$\begin{aligned} A_0 \quad &= \quad \frac{P}{2ab^2 L_0 K}, \; a \quad = \quad \sqrt{1+\alpha^2}, \; b \quad = \quad \sqrt{1-\alpha^2} \\ \alpha \quad &= \quad \frac{v_0}{v_{crit}} \quad \text{with} \quad v_{crit} \quad = \quad \sqrt{\frac{2}{\rho A}} \cdot [EI \cdot K]^{1/4} \end{aligned} \tag{16}$$

where v_{crit} is the critical train velocity. If one now draws equations (11), (14) and (15) – with-

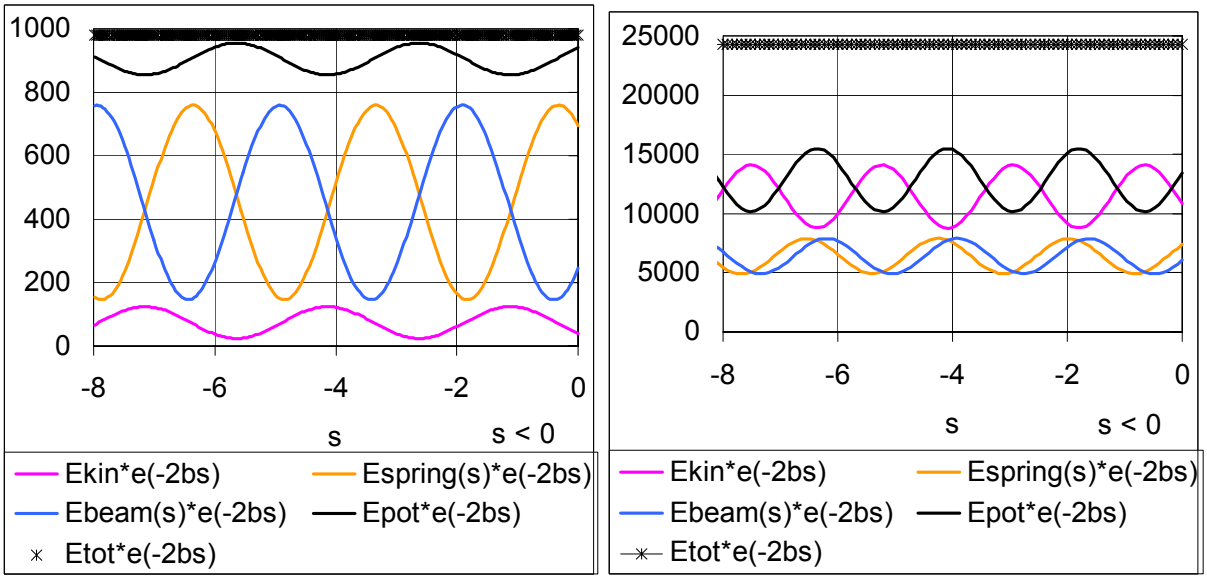

Figure 2: Energy portions of Winkler beam without dissipation for a speed of 100 km/h or $v_0/v_{crit} = 0.29$ (left) and 330 km/h or $v_0/v_{crit} = 0.94$ (right).

out the exponential expression – over the dimensionless variable s, figure 2, one can observe the interaction of the individual components: the load is at s = 0. Starting from this point, the beam transfers load (i.e. E_{pot}^{B} reduces) and the soil absorbs energy (i.e. E_{pot}^{K} increases). The potential energy falls and the kinetic energy increases. At low speeds the potential energy is much lower than the kinetic energy. The kinetic energy approaches the value of the potential energy near the critical speed. The sum of the potential energy and the kinetic energy is constant, it is, however, dependent upon the speed. At low speeds the two potential energies move in opposing directions, i.e. the beam releases energy while the subgrade load increases. These movements are increasingly in phase when the speed approaches the critical speed; for example, both transfer energy approximately simultaneously, figure 2 (right).

4.3 Energy Balances Derived from Measurements – Time Series

Equations (6), (12) and (13) comprise deflection w, particle velocity dw/dt, and acceleration d^2w/dt^2. These variables are known of from the calculations of train passages using the Winkler beam model or from passage measurements. It may also be assumed that the properties of the Winkler beam are known (even when working with measured values from passages measurements). Using the formula corresponding to equation (6) ,

$$\frac{dE_{kin}}{dt} = \frac{1}{2} \cdot \rho A \cdot \left\{ \frac{dw(t)}{dt} \right\}^2 \tag{17}$$

and the law of substitution, applied similarly to equation (8),

$$v_0 \int f(t)\ dt = \int f(x)\ dx \tag{18}$$

one arrives at the following rules for the kinetic energy:

$$E_{kin} = \frac{1}{2} \cdot \rho A \cdot v_0 \int \left\{ \frac{dw(t)}{dt} \right\}^2 dt \tag{19}$$

Similarly, from equations (12) and (13), one has for the potential energies

$$E_{pot}^{K} = \frac{1}{2} \cdot K \cdot v_0 \int w(t)^2\ dt \tag{20}$$

and

$$E_{pot}^{B} = \frac{L_0{}^8 K^2}{32EI \cdot v_0{}^4} \cdot v_0 \int \left\{ \frac{d^2w(t)}{dt^2} \right\}^2 dt \tag{21}$$

4.4 Energy Balances Derived from Measurements – Frequency Domain

Using a Fourier transformation a time series, e.g. x(t) can be transformed into the frequency domain, giving X(f). According to the *Parseval theorem* (e.g. Buttkus 1991) the energy (total power) of a time series x(t) can correspondingly be determined from X(f):

$$\int_{-\infty}^{+\infty} |x(t)|^2\ dt = \int_{-\infty}^{+\infty} |X(f)|^2\ df \tag{22}$$

5 PARAMETER STUDIES OF ENERGY BALANCES WITH THE WINKLER BEAM MODEL

We used the model for the Winkler beam without viscosity. The beam parameters correspond with those of a single DB track (Höhn et al. 2002). A full train is simulated for the passage (without locomotive), comprising either wagons with two-axle bogies (Facns 133, axle load

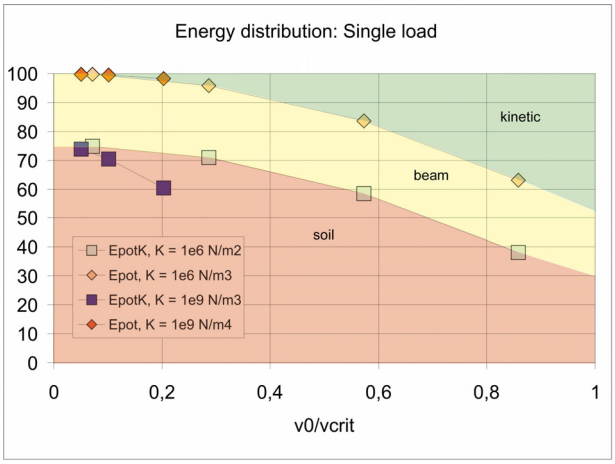

Figure 4: Distribution of energy portions for single load and two different subgrade moduli.

225 kN) or wagons with three-axle bogies (Faals 1151.1, axle load 250 kN). Two subgrade moduli are assumed for the subgrade, i.e. 10^6 N/m^2 for very soft and 10^9 N/m^2 for relatively firm soil. The determinant variable here is, however, not the subgrade modulus but the ratio of the train and the critical speed, v_0/v_{crit}.

A first step is to determine results for the single moving load case for various values of v_0/v_{crit} in order to generate a lower limiting curve. This lower limiting curve can be taken as a guide value for very slow or very light trains. The diagrams in figures 4 and 5 set total energy to 100%. The portion below the „EpotK“ curve is designated the energy portion entering the soil. The portion between the EpotK and Epot curves represents the energy portion in the beam and the portion above the Epot curve indicates the portion of kinetic energy, figure 4.

In accordance with our model the beam is associated with the superstructure and the modulus of subgrade reaction with the subgrade. For a single load (figure 4) the predominant portion of the energy transfers into the subgrade. The kinetic energy only becomes noticeable at higher speeds. A firm subgrade (large subgrade modulus) results in the beam or superstructure having to absorb a larger percentage of the energy. This means a firm subgrade transfers more potential energy into the beam than a soft subgrade.

Figure 5 shows the same type of application for the two different goods wagons of type Facns 133 (two-axle bogie) and Faals 151.1 (three-axle bogie). In this case the portion of potential energy represents a larger share of the total energy compared to a single load. The subgrade transfers an even larger share than for a single load. The three-axle bogie is slightly more favourable for the superstructure and less favourable for the subgrade.

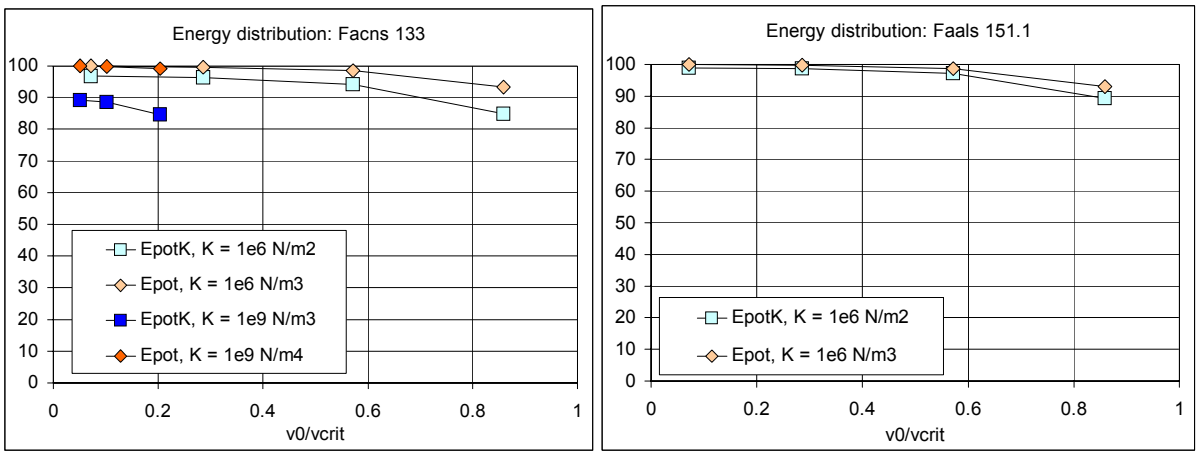

Figure 5: Distribution of energy portions for two and three-axle bogie wagons.

6 ENERGY BALANCE OF MEASUREMENT RESULTS

Figure 6 illustrates the development of the kinetic and potential energy for deterministic portions from both model and measurement as well as for stochastic portions from measurements. The trains measured comprise local passenger trains. Their deterministic portion approximates the lower limiting curve of the model calculations since their axle load is less than 225 kN. Their stochastic portions (estimated using the high pass filter) are above the deterministic values in both cases. This demonstrates that the stochastic portions of the movement variables generate noticeable portions of the kinetic energy, and therefore cannot be neglected compared with the deterministic values.

It is not the kinetic but rather the potential energy which makes the stochastically-induced energy portions so crucial. In order to determine cause and effect in more detail, figure 7 shows the respective components of the potential energy. The stochastic portion in the subgrade is approximately equal to the deterministic portion. In contrast, in the beam the stochastic portions dominate. Consequently the effect of the higher frequency loads is much more critical on the beam than it is on the subgrade.

Figure 8 investigates the energy distribution for the measured time series similar to figures 4 and 5: in the case of the deterministic portion the evaluated measurements transfer energy into the subgrade as well as into the beam. In contrast to the model calculations for the freight trains, less energy is absorbed by the subgrade in the case of the passenger train passages measured. The beam has to absorb a major portion. The picture is simple for the stochastic portion: virtually all energy is absorbed by the beam.

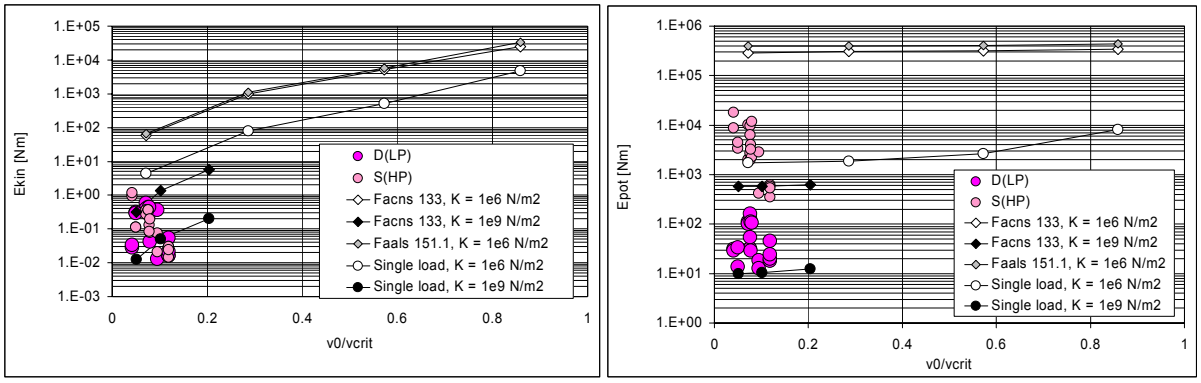

Figure 6: Kinetic energy (left) and potential energy (right) from model calculations and measurements.

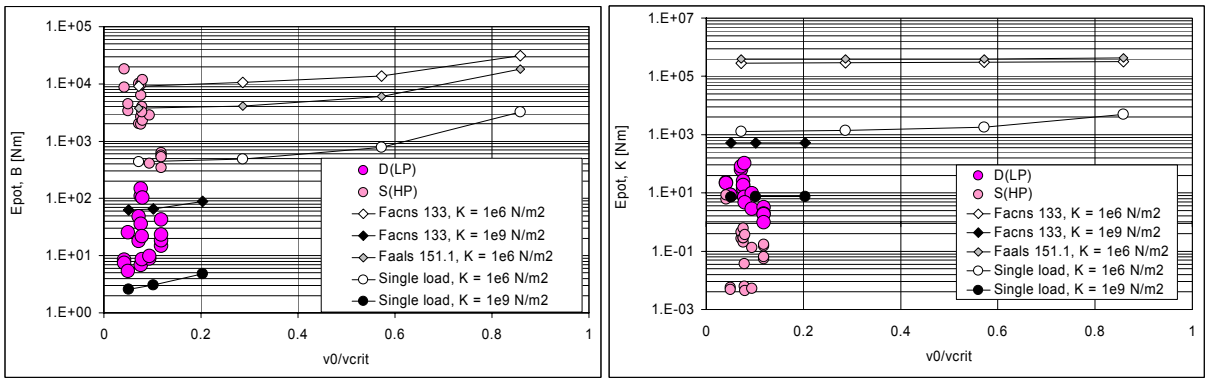

Figure 7: Potential energy from model calculations and measurements. Left: potential energy in the beam. Right: potential energy in the bedding.

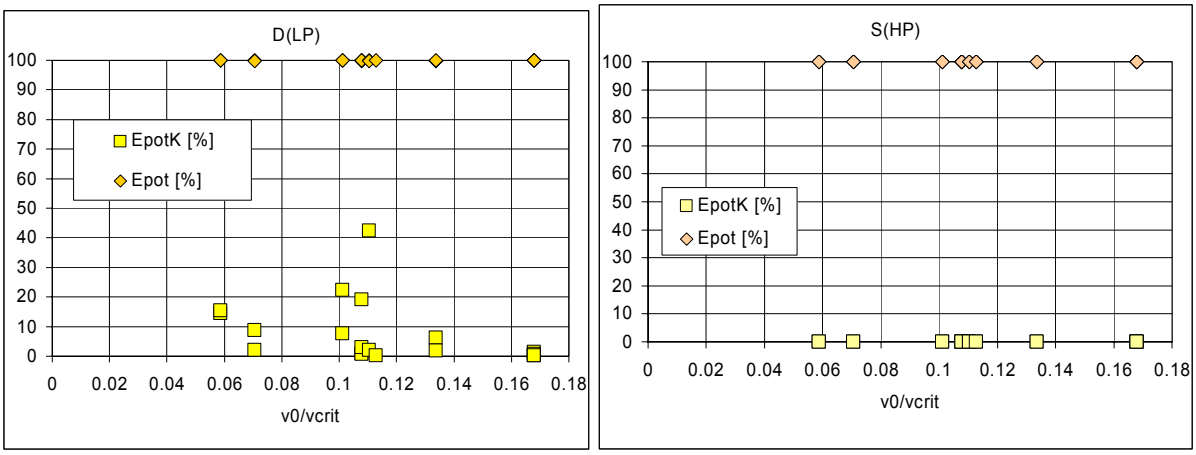

Figure 8: Distribution of energy for deterministic (left) and stochastic (right) portions of the measured movement variables.

7 DETERMINATION OF ADDITIONAL LOADS

As long as the train velocity is far below the critical velocity of the track, static and deterministic dynamic deflections are about the same. In this case, only stochastic vibrations contribute to "additional dynamic loads" (additional, in the context of Superstructure Design (Deutsche Bundesbahn 1992), relates to the static load):

$$P_{add}\left(v_0 << v_{crit}\right) \approx 2\,L_0 K \max\left|w_s\right| \tag{23}$$

where w_s is the stochastic part of the deflection. It is apparent in the evaluation of the measurement results that the additional loads determined can be larger by up to a factor of 2 than assumed for the Superstructure Design (Lieberenz et al. 2002, Deutsche Bundesbahn 1992).

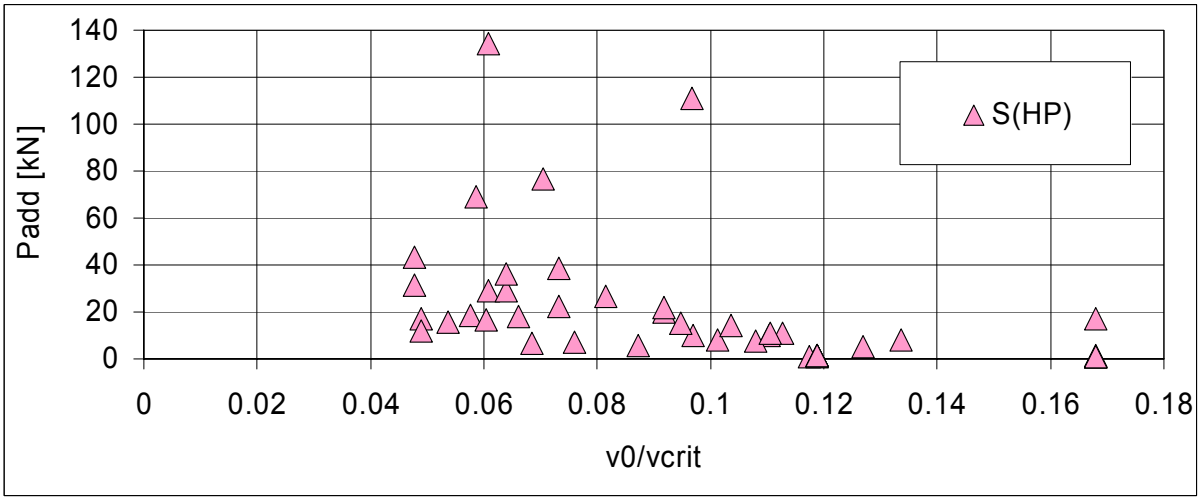

Figure 9: Dynamic additional loads determined from the stochastic portion of the movement variables.

8 CONCLUSIONS

A distinction is made between deterministic (low frequency) loads caused by the train geometry and stochastic (i.e. high frequency) loads caused by irregularities of the train or the track. The respective portions are determined from the measurements using low pass and high pass filtering with the same cut-off frequency. The assumption is made that the deterministic portion is best described using a Winkler beam model.
It is postulated that the damage criteria or stability assessments for railway tracks depend upon the frequency range of the load. It was decided that assessment criteria could be best developed with an analysis of the vibrations induced by the passage of trains. To this end the potential energy in the superstructure and the subgrade as well as the kinetic energy were determined. The procedure adopted is demonstrated using a Winkler beam model. Parameter studies are used to investigate the energy transfer in the Winkler beam for goods wagons with two and three-axle bogies respectively on hard and soft subgrades.
The evaluation of the energy balances for the deterministic and stochastic portions of the vibrations measured at the foot of the ballast produced the following results:

- Stochastic energy portions are up to 2 orders of magnitude above the deterministic energy portions.
- Stochastic energy portions are transferred almost completely into the superstructure as potential energy.
- According to the theory (Winkler beam model) almost 80 – 90 % of the deterministic energy portions transfer into the subgrade. The measured results indicate that on average 30 – 40 % of the energy transfers into the subgrade; values of up to 80 % were only measured in isolated cases. The residual energy transfers primarily into the superstructure.
- Goods wagons with the three-axle bogie represent lower stresses on the superstructure (beam) and higher stresses on the subgrade than do goods wagons with the two-axle bogie. This is due to the higher axle load of the three-axle wagon.

It may be concluded that the superstructure is primarily responsible for energy transfer. If one is principally interested in assessing the subgrade, as in the case in point, the energy investigations imply that we should focus our attention on the deterministic loads and the development of subsidence over time caused thereby. The development over time of acceleration is more crucial for the superstructure. Presenting conclusions as to the relative qualities of the axle separation etc. will only be possible after one has reliable criteria for assessing damage to tracks.
Railway track sections are designed according to the assumption of certain dynamic additional loads which are added to the static load. According to the Winkler beam model, noticeable dynamic additional loads are only generated by the deterministic portion at higher speeds (from approx. 20 – 30 % of the critical speed). Our measurements took place at speeds below 20 % of critical speed. Consequently we need only to consider the stochastic loads to determine the additional dynamic load. The maximum subsidence measured is converted into an additional load for a single moving load using the Winkler beam model. Although our measurements took place at the foot of the ballast, we arrived at values for the additional loads of up to two times the values as used in the design of superstructures.

ACKNOWLEDGEMENTS

We are grateful to Kurt Bram for providing some of the measurements analysed here. We thank Renate Pfeiffer for performing some of the numerical processing and checking the re-

sults. Her contributions are indispensable. We appreciate Frank Müller-Boruttau's readiness to discuss our results.

REFERENCES

Buttkus, B. (1991). *Spektralanalyse and Filtertheorie in der angewandten Geophysik.* Springer-Verlag, Berlin.

Dörr, J. (1948). *Das Schwingungsverhalten eines federnd gebetteten unendlich langen Balkens*. Ingenieur-Archiv 16 (5 & 6) 287-298.

Fryba, L. (1999). *Vibrations of Solids and Structures under Moving Loads*. 3rd edition, Thomas Telford, London.

Höhn, J., Göbel, I. R., Bram, K., & Meyer, H. (2002). *Determining dynamic properties of track-soil systems on soft soils by empirical and theoretical method.* 5th European Conference Numerical Methods in Geotechnical Engineering (NUMGE), 4-6 September, Presses de l'école nationale des ponts et chaussées, Paris, pp. 1025-1030.

Lieberenz, K., Müller-Boruttau, F., & Weisemann, U. (2002). *Sicherung der dynamischen Stabilität von Unterbau/Untergrund – Herangehensweise and Lösungswege an der ABS Hamburg – Berlin*. BahnBau Tiefbaufachtagung, Berlin.

Deutsche Bundesbahn (1992). *Oberbauberechnung* (*Design of superstructure,* in german). Bundesbahn-Zentralamt, München.